IOP Publishing Journal of Physics: Condensed Matter

J. Phys.: Condens. Matter **22** (2010) 084023 (14pp) doi:10.1088/0953-8984/22/8/084023

Large molecules on surfaces: deposition and intramolecular STM manipulation by directional forces

Leonhard Grill

Physics Department, Freie Universität Berlin, Arnimallee 14, D-14195 Berlin, Germany
and
Fritz-Haber-Institut of the Max-Planck-Society, Faradayweg 4-6, D-14195 Berlin, Germany

E-mail: leonhard.grill@physik.fu-berlin.de

Received 6 March 2009, in final form 10 March 2009
Published 5 February 2010
Online at stacks.iop.org/JPhysCM/22/084023

Abstract
Intramolecular manipulation of single molecules on a surface with a scanning tunnelling microscope enables the controlled modification of their structure and, consequently, their physical and chemical properties. This review presents examples of intramolecular manipulation experiments with rather large molecules, driven by directional, i.e. chemical or electrostatic, forces between tip and molecule. It is shown how various regimes of forces can be explored and characterized with one and the same manipulation of a single molecule by changing the tip–surface distance. Furthermore, different deposition techniques under ultrahigh vacuum conditions are discussed because the increasing functionality of such molecules can lead to fragmentation during the heating step, making their clean deposition difficult.

(Some figures in this article are in colour only in the electronic version)

1. Introduction

The manipulation of single molecules with the scanning tunnelling microscope (STM) enables the study of its properties in a specific, well-defined atomic-scale environment, which is not possible with methods that average over a large number of molecules. This is a very important prerequisite for a detailed understanding of physical and chemical processes at the nanoscale, but also for the development of molecular machines. Such molecules, consisting of functional components, are a fascinating challenge in molecular nanotechnology [1] and the design of such a machine requires an elementary knowledge of its mechanical motion [2]. The scanning tunnelling microscope [3] allows us not only to characterize and precisely image a single molecule and its surrounding area on a surface with sub-molecular resolution but also to obtain information about its electronic and vibrational structure. Moreover, it can act as a tool to manipulate single molecules (and atoms) and thus to probe their functions [4–8]. Such an STM manipulation, for the first time reported by Eigler and Schweizer in 1990 [9], allows the controlled displacement of single atoms [10, 11], molecules [6, 12, 13] or molecular assemblies [14, 15] on a surface and consequently the construction of nanostructures or 'writing' at the atomic scale [9, 16]. Experiments show that various mechanisms and interactions can drive the manipulation processes. Molecular displacement or conformational changes within a molecule can be achieved by interatomic forces between the STM tip and atom or molecule [6, 10, 17]. The applied bias voltage in the STM junction causes a huge electric field, due to the small electrode distance. It has been shown that this electric field can, for instance, cause diffusion [18, 19] or desorption [20] of molecules adsorbed on surfaces.

This review focuses on the deposition and the intramolecular manipulation of organic molecules on surfaces under ultrahigh vacuum conditions. These molecules carry specific (e.g. mechanical or electronic) functions and are thus rather large. Manipulation experiments are done at cryogenic temperatures around 7 K. Low temperatures are advantageous for such experiments, which require the suppression of thermal motion of atoms and molecules and high experimental stability. The intact deposition of large molecules under such ultrahigh vacuum conditions is not a trivial task, because the conventional heating procedures—for sublimation or evaporation—require rather high temperatures. Hence, the deposition step is essential in such experiments and is therefore discussed

separately in section 2, while manipulation experiments are presented in section 3.

The manipulation experiments are done by direct chemical or electrostatic forces between tip and molecules. They cause, in contrast to a lateral dislocation on the surface [21], changes of the internal molecular structure such as, for instance, the rotation of a molecular side group, changes in the bond angles or isomerization. These processes can be accompanied by modifications of the physical or chemical properties, which render the investigation of such elementary processes at the single molecule level highly interesting.

Inelastic electron tunnelling processes would exceed the scope of this review and are not discussed. In these processes, the tunnelling electrons (forming the current that is flowing between tip and sample) are inelastically scattered and lose energy, which can enable intramolecular manipulation [22]. In this way, various changes can be induced, such as, for instance, molecular rotation [23, 24], molecular vibration [25], bond rotation [26], isomerization [27], conformational changes [28] or chemical reactions [29–33].

2. Deposition of large molecules

An important step in the STM manipulation of functionalized molecules is their deposition onto surfaces under ultrahigh vacuum conditions, where intact molecules adsorb in an atomically clean environment. The temperature of the sample during this deposition determines the diffusion and therefore the growth mode of the molecules. This is of particular importance for surfaces with very low diffusion barriers, such as, for instance, NaCl films. The deposition of rather small molecules (the diffusion barrier typically increases with the molecular size) onto thin NaCl films therefore requires very low sample temperatures [34]. This condition can only be met if deposition is done directly in the low temperature STM chamber and thus requires specific chamber set-ups, where the molecular evaporator has access to the cooled STM part [35, 36]. The most common deposition method is based on evaporation or sublimation (depending on the vapour pressure and melting point of the molecules) from a so-called Knudsen cell. This cell, a small volume containing the molecular substance, is heated by a filament until a sufficient vapour pressure is achieved and the molecules leave the Knudsen cell through a hole towards the sample. Careful degassing of the cell ensures low background pressures and thus a very clean deposition.

However, any functional molecule, which is of interest for future applications in nanotechnology, will exhibit a certain complexity [37]. Hence, the molecular weight is raised due to the embedded functions. As a result, the conventional deposition of molecules from a Knudsen cell becomes difficult, because the thermal energy injected into the molecules reaches the range of the intramolecular binding energies. Beyond a specific size, the molecules dissociate rather than sublime and molecular fragments are deposited instead of intact molecules. It is therefore necessary for the investigation of large molecules to use alternative methods that allow, on the one hand, the

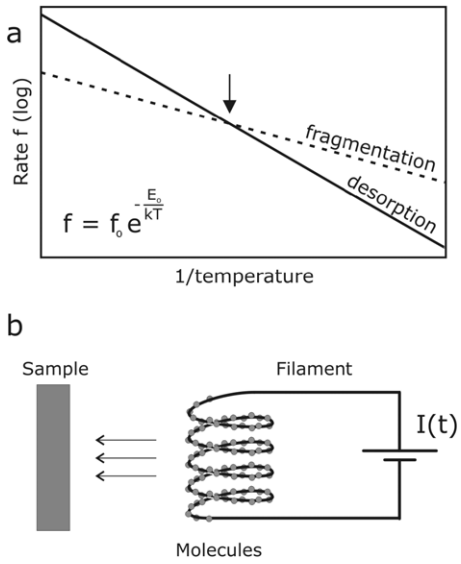

Figure 2.1. (a) Principle of the 'rapid heating' procedure. The rates for fragmentation (dashed line) and desorption (solid line) are plotted as a function of 1/temperature. The underlying equation is shown in the inset. The arrow indicates the temperature at which the desorption rate is equal to the fragmentation rate. Reprinted with permission from [40]. Copyright (2006) Elsevier. (b) Experimental set-up for the deposition of molecules onto the sample surface from a filament by applying a current pulse $I(t)$.

controlled deposition of very small coverages (in the sub-monolayer range) and, on the other hand, clean conditions.

One way to avoid, or rather suppress, molecular fragmentation during the deposition is the so-called 'rapid heating' technique [38, 39]. It is based on the idea that the fragmentation and desorption rate (in a first approximation given by the exponential function f in figure 2.1(a)) of the molecules have a different activation energy E_o and thus depend differently on the temperature. Thus, although the base rate f_o and the activation energy E_o of the two processes are unknown, it is reasonable to assume that their curves cross somewhere in the rate versus 1/temperature diagram (as marked by an arrow). Accordingly, the high temperature range offers conditions for the deposition of intact molecules, because the desorption rate overcomes the fragmentation rate. In the Knudsen cell, thermodynamic processes occur rather slowly and this high temperature range cannot be reached without dissociation of the major part of the molecules. In contrast, a very fast temperature increase would suppress this fragmentation and the conditions for relatively high desorption rates (in any case clearly larger than the fragmentation rate) are met.

Figure 2.1(b) shows the experimental set-up for this technique: a filament, which is covered with the molecules (after dipping it into a solution of molecules and subsequent drying from the solvent), is briefly heated by a current pulse $I(t)$ of several A for a period of several hundred milliseconds. If a sufficiently high temperature range is reached, intact molecules are deposited onto the sample by this method.

The deposition of molecular wheelbarrows is a challenging task, because of their large molecular weight. This complex

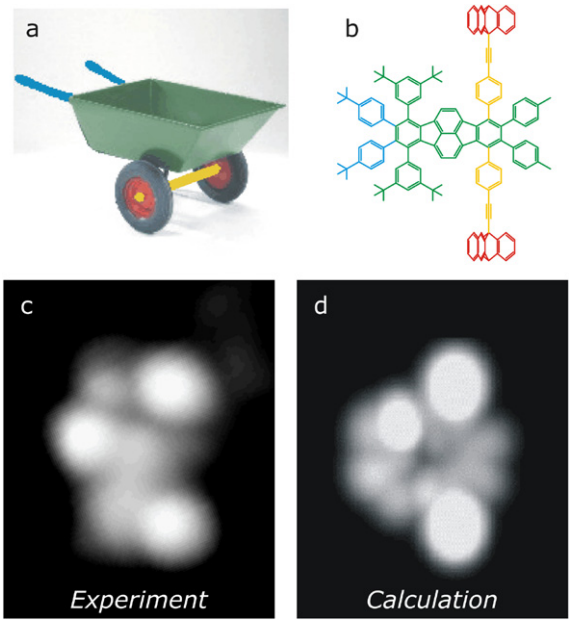

Figure 2.2. (a) Macroscopic wheelbarrow. (b) Chemical structure of a molecular wheelbarrow, the synthesis is described in [41]. The triptycene groups are acting as wheels connected by the axle. Experimental (c) and calculated (d) STM images (4×5 nm^2 in size) are in very good agreement. Reprinted with permission from [42]. Copyright (2005) Elsevier.

molecule, shown in figure 2.2, consists of a polyaromatic central platform with two wheels, which are connected by an axle. Two 3,5-di-*tert*-butyl phenyl groups, considered as two legs that should maintain the polyaromatic board away from the surface by staying perpendicular to the polyaromatic platform, are connected to the board. Furthermore, two 4-*tert*-butyl phenyl groups are added to the end of the central platform to act as handles of the barrow. The most important feature of the molecule are the wheels [43], which are able to rotate around the σ-bond (i.e. their wheel axis) so that they should enable a lateral motion of the entire molecule on the surface by rotation, in analogy with a real macroscopic wheelbarrow. During deposition from a conventional Knudsen cell (at 800 K), these molecules only fragment and no intact molecules are found on the surface [40].

If the 'rapid heating' technique (6 A for 600 ms) is used instead, intact wheelbarrow molecules can be sublimed and imaged with the STM (figure 2.2(c)). Their appearance is in very good agreement with calculated images (d) and can therefore be assigned to a particular conformation. It is dominated by the characteristic features of the molecule: two lobes assigned to the triptycene wheels and another bump (on the left side of the image) from one of the 3,5-di-*tert*-butyl phenyl groups. The relatively large size of these groups (see figure 2.2(b) is the reason why they dominate the images. The conformation of the molecule in figure 2.2(c) is the most common on the surface, but—as the molecule is rather complex—there also other stable conformations, which could be identified on the surface [42].

Although the purity of the wheelbarrow molecules after synthesis [41] was determined to be higher than 99.5%, a side-product could be detected by mass spectrometry: two triptycene wheels connected by a C≡C–C≡C linker (a so-called 'wheel-dimer' [43]), which are observed in the STM images. Interestingly, the presence of these low molecular weight contaminants leads to cycloaddition reactions on the metallic surface, which acts as a catalyst [40]. As a result, highly symmetric trimer and tetramer molecules are formed *in situ*. Their chemical structure is revealed from a comparison with STM image calculations. The observation of this chemical reaction shows that large nanomachines, which exhibit a variety of functional subunits, must be deposited very carefully in order to avoid the formation of side products.

Even though the 'rapid heating' technique suppresses molecular fragmentation and thus extends the molecular weights that can be deposited intact onto surfaces, it still includes heating of the molecules at the sublimation stage. This is not the case for the so-called pulse valve technique, which was successfully used for the deposition of large molecules such as DNA [44], polymer chains [45, 46], carbon nanotubes [47, 48] and nanocrystals [49]. The experimental set-up is presented schematically in figure 2.3(a). The molecules are deposited in a solution from air atmosphere onto the sample kept under UHV conditions. The solution is not exposed to any heating procedure, thus avoiding any thermal dissociation of the molecules, a clear advantage to the methods discussed above. The valve, which has a small orifice of about 50 μm, is opened for very short periods in the millisecond range and the saturated solution enters into the chamber.

The role of the solvent becomes important if rather small molecules are deposited where their size reaches the order of the solvent molecules. In most of the studies done with small molecules in the past, STM images have been taken at room temperature, so that the solvent is not resolved and appears as fuzzy lines (due to its high mobility) [50]. Recently, the preparation by pulse injection has been investigated for the first time with a low temperature STM, working at cryogenic temperatures of 8 K, where the diffusion of the solvent molecules is frozen [51]. Hence, the cleanliness of the substrate (after solvent desorption) can be studied.

The molecules chosen for this study were Cu-tetra-3,5-di-*ter* butyl phenyl porphyrin (Cu-TBPP) molecules. They consist of a central porphyrin ring and four phenyl-based lateral groups, which act as 'legs'. The legs can rotate around their σ-bond, leading to characteristic conformations on metal surfaces therefore and appearances in STM images [52]. At large coverages, Cu-TBPP islands are formed by self-ordering processes, where molecules grow according to their chemical properties [53]. The cleanliness of such a layer is of fundamental importance as contamination within an island would perturb the periodicity and deform the structure.

Directly after deposition (six pulses with 116 ms opening time each), disordered structures were observed in the STM images and no Cu-TBPP molecules could be identified [51], which was explained by the large amount of solvent present on the surface (note that the number of adsorbed solvent molecules is probably much larger than that of Cu-TBPP). Subsequently, soft annealing to 220 °C (for 5 min) was used to clean the surface from the solvent, whereas the molecules

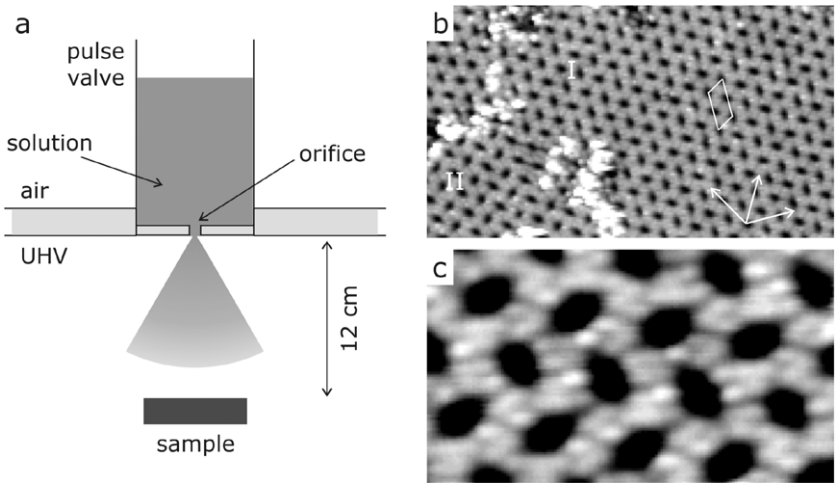

Figure 2.3. (a) Scheme of the molecular injection using a pulse valve. The clean sample is positioned in front of the valve at a distance of about 12 cm. (b) STM image (43×24.3 nm^2, $U = 0.8$ V, $I = 80$ pA) of the Cu(111) surface covered with Cu-TBPP molecules. The unit cell (20×35 Å^2) is marked by a rhombus. Different domains of the structure are named I and II. The symmetry directions of the Cu(111) substrate are indicated by arrows. (c) Enlarged view of the same structure (8.9×5.1 nm^2, $U = 0.8$ V, $I = 80$ pA) where only the *tert*-butyl legs contribute to the contrast. Reprinted with permission from [51]. Copyright (2006) Elsevier.

do not desorb. STM images of the resulting surface structures show highly ordered molecular layers (figures 2.3(b) and (c)), which completely cover the surface. Each molecule consists of eight lobes, which reflect the spatially extended *tert*-butyl groups (two attached to each of the four phenyl rings), while the central porphyrin ring is not visible (due to the smaller height and, in particular, to the electronic decoupling from the surface by the legs), in good agreement with experimental results and calculations of single molecules [52]. The molecules therefore lie flat on the surface, having all phenyl rings parallel to the substrate, when adsorbing in a complete layer. This appearance has been proven by comparison with results obtained by deposition from a conventional Knudsen cell [51].

Although the molecular layers reveal a very high order and perfect cleanliness, small amounts of contaminants were found at the boundary between different ordered domains (as in figure 2.3(b)). These boundaries offer energetically preferred adsorption sites to contaminants or rest solvent molecules, as they accumulate in these regions or at step edges. Note that no solvent molecules are visible on the ordered layer, although their diffusion is suppressed at the low temperature of 8 K of the present measurements. This demonstrates the cleanliness of the molecular structure over large areas of several hundred Å, limited by domain boundaries or step edges.

This pulse valve technique is a very suitable method to deposit large functionalized molecules, because the experimental set-up is rather simple. However, a precise control of the molecular coverage is not straightforward and presumably depends on the formation of small droplets at the orifice during the valve opening. A more complex method is the electrospray deposition in vacuum where the molecules are not directly deposited from the solution, but from a solution mist [54, 55, 57, 58]. This method, which is presented in figure 2.4(a), requires much more experimental effort, because the molecular beam passes several chambers of different background pressures. In this way, a pressure during deposition is obtained, which is several orders of magnitude lower than that during deposition by a pulse valve [59]. Furthermore, it has been shown that the composition of the created molecular beam can be analysed in an elegant way by time-of-flight mass spectrometry [60].

This electrospray deposition technique involves the formation of molecular ions at the emitter tip (E), which is held at a high voltage. When these ions are hitting the sample, the spray current is determined as a measure of the molecular flux. The tip–sample distance is usually minimized for an optimal flux, but still allowing complete desolvation. Similar to the pulse valve technique, there is no size limit for the molecules and the only limit is given by the solubility of the molecules. Recently, it has been shown that the electrospray deposition is even non-destructive for a previously prepared hydrogen-bonded supramolecular network on the surface, which maintains its structure upon deposition of additional fullerene molecules [55].

An example of this technique is presented in figure 2.4(b), where fullerene molecules were deposited onto an Au(111) surface [58]. Due to their high mobility on the surface, decoration of the step edges by these molecules is observed. For comparison, the same electrospray preparation was repeated with a pure solution, i.e. without fullerene molecules (figure 2.4(c)). After spraying for the same duration and in the same sample position, no features are observed at the step edges, which confirms that the step decoration was due to C_{60} and not solvent molecules. A further development in the electrospray method consists of the additional use of a quadrupole for mass separation at the end of the pumping stages [56]. By applying different voltages to the rod pairs of the quadrupole, the mass-to-charge-ratio of the molecular ions can be chosen within a well-defined range. In this way, the molecules that pass the quadrupole can be selected by their mass and small fragments can be sorted out [56]. After

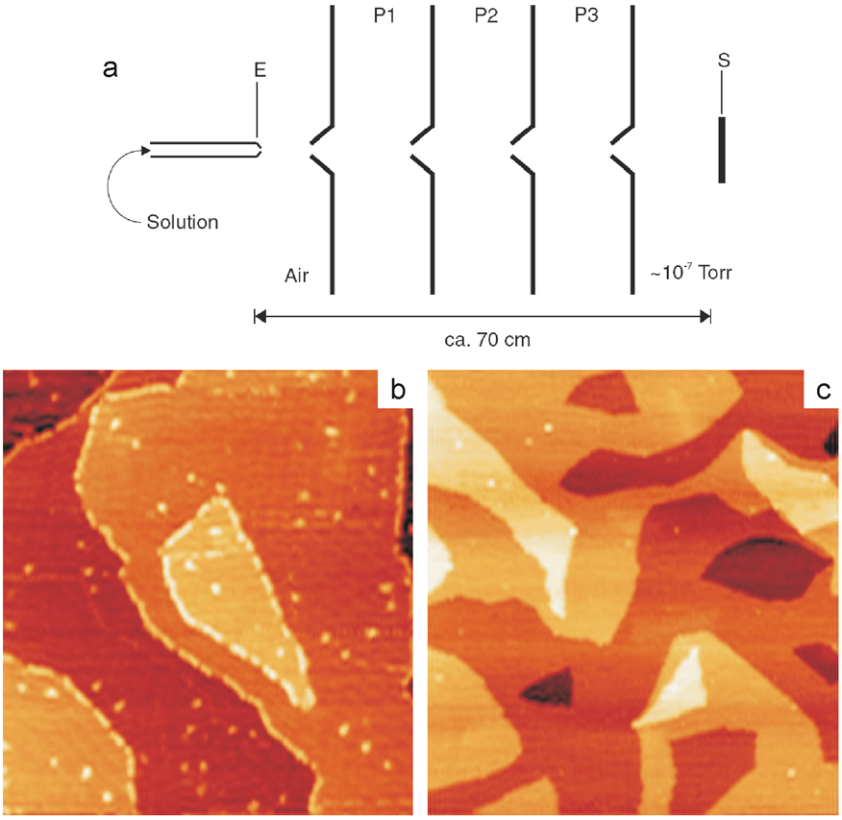

Figure 2.4. (a) Schematic illustration of the electrospray system with the emitter tip (E) at ambient pressure and differentially pumped stages (P1–P3). The sample surface (S) is in the low 10^{-7} Torr range during operation. (b) STM image (107.8 nm × 117.6 nm, −0.70 V, 0.03 nA) after electrospray deposition of C_{60} molecules. (c) STM image (220 nm × 240 nm, −1.80 V, 0.03 nA) after 1 h electrospray of only the solvent (toluene/acetonitrile mixture). Reprinted with permission from [58]. Copyright (2007) Institute of Physics.

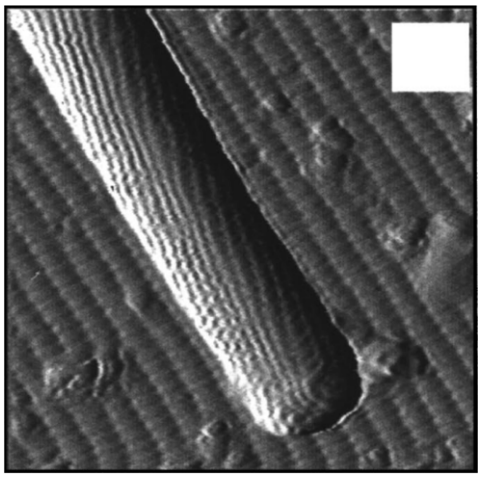

Figure 2.5. STM image (10 nm × 10 nm), showing a single-walled carbon nanotube physisorbed on an atomically resolved Si(100)-2 × 1:H surface. Reprinted with permission from [61]. Copyright 2003 American Institute of Physics.

leaving the quadrupole, the mass-selected molecules reach the deposition chamber.

A 'dry', i.e. solvent-less, deposition technique has been developed for carbon nanotubes, where the use of a solution can create structural damage [61]. This so-called 'dry contact transfer' is performed *in situ* and can be used for nonvolatile and insoluble molecules [62]. A fibreglass sheath is first covered macroscopically with nanotube powder and then transferred into ultrahigh vacuum. After degassing the sheath *in situ*, it is brought into direct contact with the clean, freshly prepared surface at room temperature. Figure 2.5 shows a single carbon nanotube end that has been deposited on a hydrogen-terminated Si(100) surface by dry contact transfer. Both the nanotube and the surface can be resolved atomically (the chiral structure of the nanotube can be clearly seen), showing that this method is accompanied by a rather low level of contamination. Moreover, carbon nanotubes can be primarily found isolated by this method [62], facilitating their investigation by local probe techniques. Although this method is suitable for carbon nanotubes where the intact ends of single long nanotubes can be observed (figure 2.5), it seems less attractive for other, short, molecules where the molecules probably adsorb in huge clusters and it might be very difficult to find entire molecules in an intact surface area.

3. Intramolecular manipulation

The controlled manipulation of single molecules on surfaces with the tip of a scanning tunnelling microscope is of great interest for a detailed understanding of the molecular functions. Intramolecular conformations or molecular

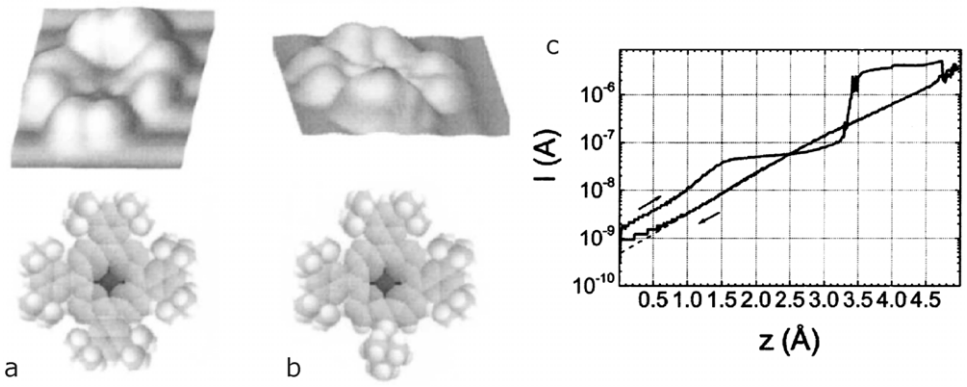

Figure 3.1. (a, b) STM images (upper panel) and calculated molecular structures (lower panel) of a Cu-TBPP molecule on Cu(211) in two conformations: lying flat on the surface (OFF state; (a)) and having one leg rotated out of the porphyrin plane (ON state; (b)). (c) $I(z)$ curve recorded during the controlled rotation of a leg from the ON leg to the OFF leg state with $z_o = 7$ Å. A sample voltage of 1 V has been applied during this $I(z)$ cycle. The arrows indicate the approach and retracting steps (see text). Reprinted with permission from [66]. Copyright (2001) by the American Physical Society.

adsorption positions/geometries can be achieved on a surface, which often would not be present after sample preparation, because they are energetically not favoured [63, 64]. At cryogenic temperatures (where molecular manipulation is usually done) instead, molecular configurations are 'frozen' due to the small thermal energy available. Furthermore, manipulation experiments not only give detailed insight into the molecular configurations and motions on a surface, but represent also a very interesting set-up for the study of interatomic forces (between STM tip and molecule) at atomic-scale distances. The various forces, active in such a junction, can in a first approximation be described by the Lennard-Jones potential (as a function of the interatomic distance between two noble gas atoms), consisting of attractive van der Waals [65] and repulsive interactions (Pauli repulsion). The repulsive forces can, in contrast to the attractive ones, become very large at small interatomic separations. In the case of STM manipulation, chemical interactions and the role of the tunnelling current and the applied electric field must be taken into account. These forces can be studied during manipulation with high spatial precision if the relevant parameters (lateral and vertical tip position, applied bias voltage and tunnelling current) are systematically modified.

For intramolecular manipulation experiments, molecules with several clearly defined conformations, which give rise to different appearances in STM images, are desired. In this way, the achieved changes in the images before and after the manipulation experiment can be characterized. This is the case at low temperatures where spontaneous modifications can be excluded, while at elevated temperature thermally induced spontaneous conformational changes can occur, for instance between different enantiomers [67]. Figure 3.1 shows manipulation experiments with Cu-tetra-3,5 *di-ter-butyl-phenyl* porphyrin (Cu-TBPP) molecules on a Cu(211) surface [66]. These molecules consist of a central porphyrin ring and four *di-ter-butyl-phenyl* legs that are attached laterally. Each of the legs is able to rotate around its σ-bond out of the porphyrin plane, resulting in two characteristic conformations of each leg, shown in figures 3.1(a) and (b). The rotated leg, i.e. the ON state, appears in (b) higher than the other ones (in the OFF state flat on the surface), due to the modified configuration.

Various manipulation experiments, moving the tip laterally across the molecule or approaching it vertically, could show that it is possible to induce the rotation of a single leg with the STM tip. Figure 3.1(c) shows the current during a vertical manipulation, where the tip is approached from a height of 7 Å above the surface (the vertical feed z is plotted on the x axis). The approach curve (from left to right) reveals various features that can be assigned to the different stages of a leg rotation. In the beginning, the current grows exponentially, due to the tip approach through vacuum, until the molecule is in van der Waals contact with the tip (at about 1.7 Å) and a plateau is visible. The constant current in this plateau region (around 2.5 Å) is due to the rotation of the leg under the influence of the tip until it reaches the planar orientation (and the current increases again). Hence, the tip is pushing a single leg downwards as a result of the repulsive forces between tip and molecule at small distances, bringing it from the ON to the OFF state, while the rest of the molecule remains unchanged. This conformational change is confirmed in STM images that are taken afterwards. On the other hand, the retraction curve (from right to left in figure 3.1(c)) is a straight line. This exponential decay is characteristic for a tunnelling junction and shows that the leg is not pulled upwards and the manipulation is not reversible. A similar experiment, rotating a molecular group within a molecule, has been done with molecular wheel-dimers where one of the two wheels is rotated under the influence of the STM tip [43]. Due to the nature of the molecule and its adsorption configuration, this intramolecular conformational change leads, as intended, to the rolling of the entire wheel-dimer molecule.

Porphyrin molecules are very suitable for intramolecular manipulation experiments, not only because of the possibility to attach molecular side groups and to rotate these groups as presented above. The porphyrin ring itself can have various conformations, planar and non-planar ones [69]. In an experiment by Ho and co-workers [68], the internal

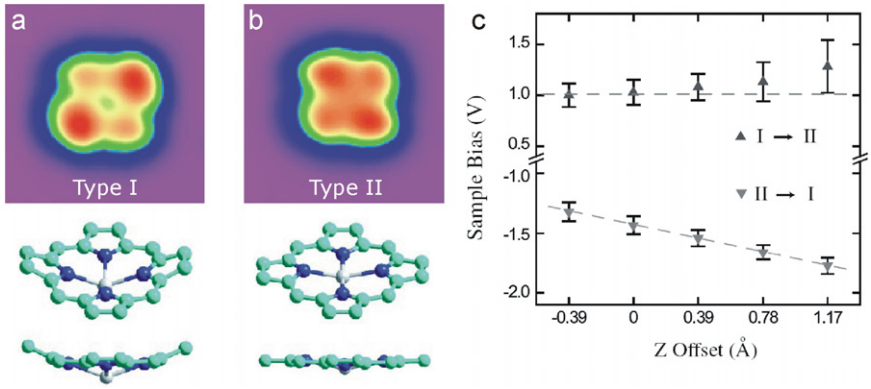

Figure 3.2. (a) STM images (33 × 33 Å^2) and (b) corresponding schematic views of 1,3,5,6-tetramethyl-2,4,6,8-tetraethylporphyrine zinc (II) molecules (ZnEtioI) adsorbed on an NiAl(110) surface in two conformations, called type I and II. (c) Variations of threshold voltages to undergo a reversible conformational transition from type I to type II or from type II to type I as a function of the change in tip–substrate separation. Reprinted with permission from [68]. Copyright (2004) by the American Physical Society.

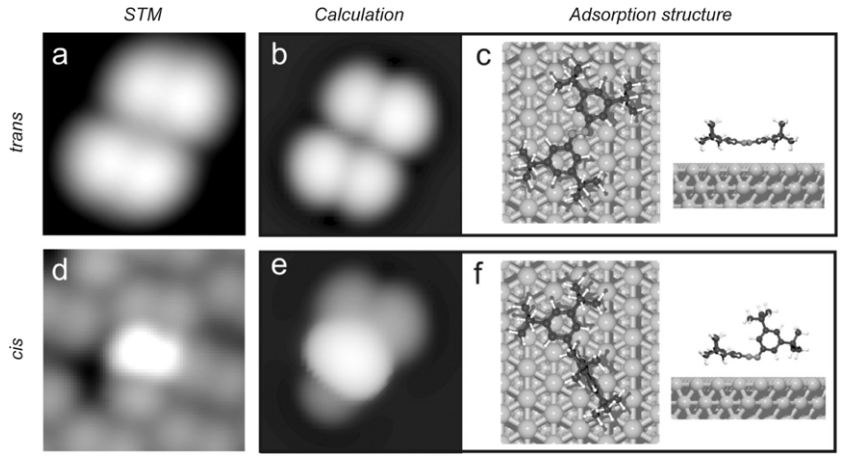

Figure 3.3. (a) Experimental and (b) calculated STM images (24 × 24 Å^2) of a meta-TBA molecule in the *trans* form on Au(111) with the corresponding adsorption structure (c) in a front view (left) and in a side view (right). The lower panels (d)–(f) show experimental and calculated STM images (24 × 24 Å^2) and the adsorption structure of the molecule in the *cis* form. Reprinted with permission from [27]. Copyright (2008) American Chemical Society.

conformation of the central porphyrin ring is modified by intramolecular manipulation, going from a bowl-like configuration (type I in figure 3.2(a)) to a planar one (type II in (b)) and vice versa. The corresponding change of the molecular appearance can be clearly seen in STM images. The driving force for these conformational changes is determined by analysing the variation of the threshold voltage as a function of the tip height (figure 3.2(c)). While the transition from type I to type II is caused by inelastically scattered tunnelling electrons, the transition from type II to type I (lower dataset in (c)) shows a linear relationship between voltage and tip–surface distance. This linearity reveals that a constant electric field (of 0.26 V Å^{-1}) is required to induce the conformational change and thus that the intramolecular manipulation is driven by the electric field in the STM junction.

Another example for intramolecular manipulation concerns molecular switches that undergo a reversible transition between stable states with characteristic physical or chemical properties [70]. The manipulation induces here not simply a conformational change, but an isomerization of the molecule (between *trans* and *cis* isomers) that is accompanied by changes in its electronic structure and optical properties. Such isomerization processes are well studied in solution, where the switching is typically achieved by illumination with light (photo-isomerization) [71]. Figure 3.3 shows for 3,3′,5,5′-tetra-*tert*-butyl-azobenzene molecules (meta-TBA) that such processes can also be induced with an STM tip on an Au(111) surface (photo-induced switching has recently also been observed for the same system [72, 73]). After deposition, the molecules are found in the *trans* state in highly ordered islands, due to their mobility at room temperature (a single molecule is presented in the upper panel of figure 3.3). The *cis* conformation (lower panel; a molecule within an island is visible in (d)) can be achieved experimentally by applying voltage pulses [27, 74, 75]. Note that this process is reversible, restoring precisely the initial appearance of a molecule after an entire switching cycle (from *trans* to *cis* and back to *trans*) by applying voltage pulses. Detailed analysis shows that it is, under certain conditions, driven by the electric field in the

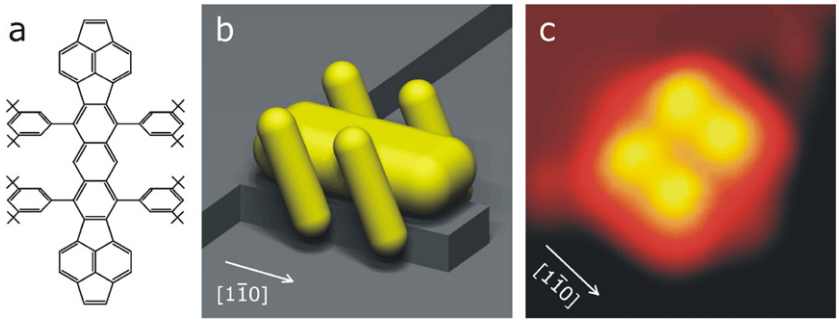

Figure 3.4. Chemical structure (a), scheme (b) and STM image (35×35 Å^2; $I = 0.2$ nA and $U = 1$ V) (c) of a reactive Lander (RL) molecule adsorbed on a Cu(110) nanostructure (always oriented in [1$\bar{1}$0] direction). (b) Adsorption geometry of RL molecules on the Cu nanostructure (in the 'parallel legs' conformation). Reprinted with permission from [78]. Copyright (2006) American Chemical Society.

STM junction [74]. The good agreement between the STM ((a) and (d)) and the calculated images ((b) and (e)) confirms that the observed changes are due to isomerization processes. The molecular structures of the planar *trans* and the non-planar *cis* isomer on the surface (figures 3.3(c) and (f)) are very different, similar to their structures in the gas phase [76]. Scanning tunnelling spectroscopy measurements have shown that their electronic structure is also modified during isomerization as an unoccupied molecular orbital is found at lower energies for the *cis* than for the *trans* isomer. Such energetic shifts of molecular orbitals are expected and absorption spectra of these meta-TBA molecules in solution exhibit absorption bands at different positions for the two isomers, which is characteristic for azobenzene derivatives [74]. Note that the direct environment of each individual molecule, i.e. the surface and the surrounding molecules, can have a profound influence on the switching capability [75].

The experiments presented above show that intramolecular manipulation can be done in a very controlled way with single molecules, taking advantage of either chemical or electrostatic forces between the STM tip and the molecules. In the following, it will be shown with the so-called Lander molecules how different mechanisms can be explored with one and the same manipulation process. These molecules, synthesized by Gourdon [77], consist of a central board and four lateral 3,5-di-*tert*-butylphenyl spacers ('legs'), which lift the central board up from the substrate.

Various types of similar Lander molecules exist: the so-called single Lander (SL) ($C_{90}H_{98}$) [79–86], which has recently also been studied spectroscopically [87], and reactive Lander (RL; $C_{94}H_{98}$; shown in figure 3.4(a)) [63, 78] molecules differ only in a double bond at both end groups of the molecular wire. In the case of the violet Lander (VL; $C_{108}H_{104}$), the central part of the molecular wire is elongated, thus increasing the leg separation [88–92]. Recently, the moulding capability of the novel DAT Lander has been studied [93]. The largest member of the Lander family is the D-Lander ($C_{178}H_{190}$), having a 3.7 nm long molecular wire and eight legs, i.e. four di-*tert*-butylphenyl groups on each side of the wire [39]. Although spacer groups elevate the molecular wire, it turned out that it is not completely decoupled from the surface. A comparison of several types of Lander molecules, differing in the length of the molecular wire, showed that the

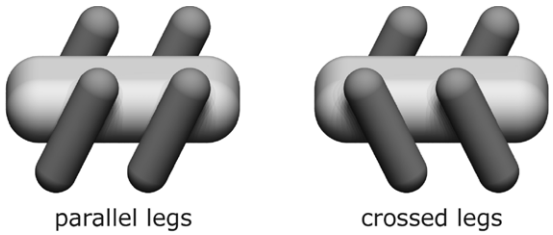

Figure 3.5. The two conformations of the Lander molecule when adsorbed on a surface: parallel and crossed legs. Reprinted with permission from [95]. Copyright (2006) Institute of Physics.

scattering pattern of the surface state electrons is dominated by the central board, which thus still interacts with the metal substrate [94].

The lateral legs of the molecules are approximately perpendicular to the central board when the molecules are not interacting with a surface or other molecules [77]. However, after adsorption on a metal surface the π-system of the polyaromatic board is pulled towards the substrate and thus the legs are rotated (around their σ-bond). Consequently, two different molecular conformations are present, the so-called parallel legs' and crossed legs' conformations (figure 3.5), where the two pairs of legs on each side of the central board are oriented in the same or in opposite directions, respectively. As a result of the steric hindrance between the butyl groups the two legs on the same side of the board are always parallel.

When STM images are taken of these molecules, the molecular appearance is mainly given by the bulky di-*tert*-butylphenyl groups. Hence, four bright lobes reflect the four legs of the molecule, while the central board contributes much less to the tunnelling current (figure 3.4(c)). Interestingly, two legs appear higher than the other two (i.e. they give a larger contribution to the tunnelling current at constant height), even though their real height above the surface is the same. This effect, which is caused by additional tunnelling channels through the molecule and has been confirmed by comparison with molecular mechanics–elastic scattering quantum chemistry (MM–ESQC [96]) calculations [80], enables the conformation from the intensity distribution in the STM image to be determined [95].

Single Lander molecules on Cu(110) are of particular interest as their adsorption causes the—thermally activated—

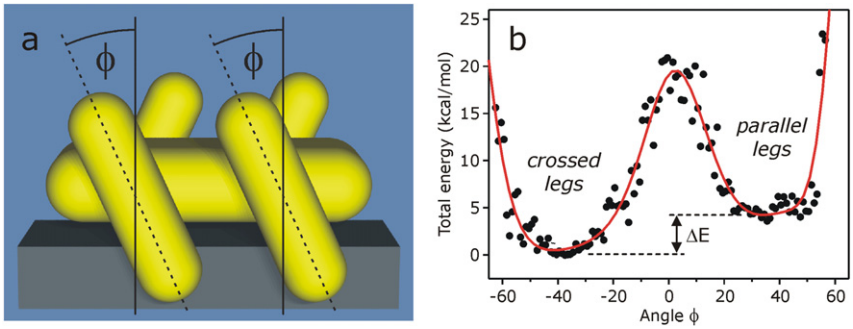

Figure 3.6. (a) Adsorption geometry of RL molecules on the Cu nanostructure (in the 'crossed legs' conformation) with the rotation angle ϕ of one pair of molecular legs indicated. (b) Calculated total energy of the molecular nanostructure copper surface system as a function of the rotation angle ϕ of one pair of legs (the solid line is plotted to guide the eyes). The two minima correspond to the 'crossed legs' ($\phi = -37°$) and 'parallel legs' ($\phi = +37°$) conformations. The curve is obtained by rotating only one pair of legs (on the same side of the central board) and leaving the other pair in the initial position. Reprinted with permission from [78]. Copyright (2006) American Chemical Society.

formation of nanostructures of copper atoms, because the molecules act as templates for the formation of a double row of copper atoms (seven atoms long) underneath them (schematically shown in figure 3.4(b)) [81]. The shape of the nanostructures, with the height of the upper substrate terrace, is thus determined by the molecules themselves. Calculations (ESQC) have shown that the central board is lifted up by the nanostructure by more than 1 Å, which reduces the steric constraint on the leg-board σ-bonds and leads to a larger distance between two opposite legs in the STM image (compared to adsorption on a terrace) [81]. After these first observations for single Landers, the deposition of reactive Lander molecules onto Cu(110) shows exactly the same phenomenon, causing copper nanostructures after removal of the molecules [63]. The same nanostructure dimensions are observed, according to the almost identical chemical composition. However, the nanostructures are nine atoms long for violet Lander molecules, due to the longer central board of the molecule [90].

This adsorption geometry is highly interesting by means of intramolecular manipulation experiments, because the central board of the molecule is lifted upwards, giving more motional freedom to the molecular legs. In such a configuration, it should in principle be possible to induce intramolecular conformational changes without dislocating the molecule on the surface, which is typically not possible for molecules that are adsorbed on a metallic terrace. The idea of the following manipulation experiments is therefore to induce a rotation of one pair of legs (i.e. switching from the crossed legs to the parallel legs' conformation or vice versa), while keeping the rest of the molecule fixed.

Calculations of the total conformational energy [85] are presented in figure 3.6. While the central molecular board and one pair of legs are kept in an unchanged position, the other pair of legs is rotated around ϕ. Two distinct energy minima are found, which correspond to the crossed and parallel legs' conformations. This intramolecular bistability of the di-*tert*-butyl-phenyl groups (legs) renders the Lander–nanostructure configuration very interesting by means of manipulation, because it should in principle be possible to rotate one pair of legs. Note that there is an energy difference of ΔE between

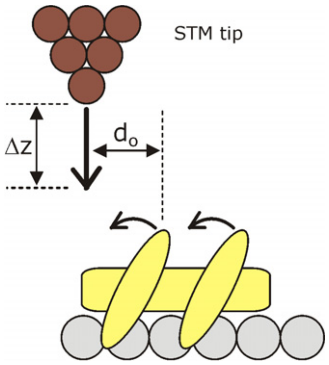

Figure 3.7. Scheme of the vertical approach manipulation process. One pair of molecular legs rotates upon approaching the STM tip. The vertical feed Δz (from the initial tip height of about 7 Å) and the lateral distance d_o of the tip from the leg (i.e. from the intensity maximum of the molecular leg in the STM image) are indicated. Reprinted with permission from [78]. Copyright (2006) American Chemical Society.

the two conformations, indicating that the manipulation from parallel to crossed legs (PL $\rightarrow$ CL) should require smaller forces than the opposite manipulation (CL $\rightarrow$ PL).

One possibility to change the intramolecular conformation is lateral manipulation, i.e. scanning the STM tip across the molecule. This can only be done if the applied forces are sufficient, but at the same time small enough to avoid lateral displacement of the entire molecule; thus the tip height must be in a suitable range [85]. Although it could be shown that in this way each pair of legs can be rotated and the molecule is switched between parallel legs and crossed legs conformations, the reliability of the process is not perfect. The pair of legs, which should be rotated, cannot be precisely chosen. Furthermore, in a few cases displacement of the entire molecule is induced. Thus, the control over the manipulation is limited.

This lack of precision is eliminated in the case of the so-called vertical approach manipulation. Figure 3.7 shows schematically the basic principle and experimental set-up of this manipulation mode: at constant bias voltage and while maintaining the lateral tip position fixed, the STM tip is

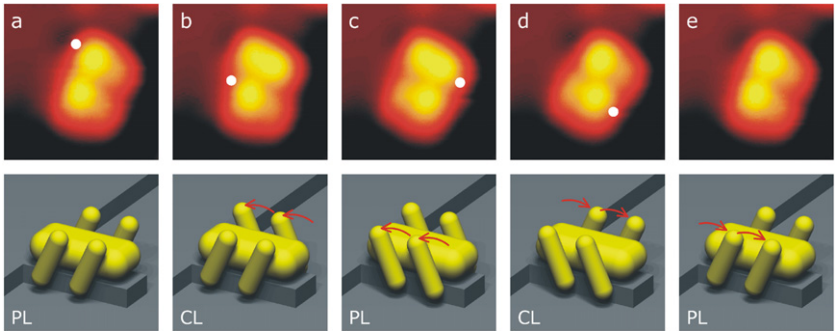

Figure 3.8. Series of STM images (upper panel), bringing one and the same RL molecule in all four possible conformations (two with parallel and two with crossed legs) by vertically approaching the tip. The lower panel shows schemes of the corresponding conformations (PL = parallel legs; CL = crossed legs). The lateral tip position of the subsequent manipulation is marked in the STM images by a white dot and the achieved conformational changes are indicated in the schemes by arrows.

approached vertically towards the molecule until one pair of legs rotates, changing the molecular conformation.

A successful manipulation shows up as an abrupt increase in the tunnelling current during the tip approach, due to the decreased tip–leg distance. Imaging the molecule afterwards confirms the successful manipulation as the desired appearance, i.e. conformation, is obtained. Note that only attractive interatomic forces can cause this conformational change, which turns out to be of great advantage (as discussed below).

A series of manipulation steps with one and the same molecule is shown in figure 3.8. Starting with the initial parallel legs (PL) configuration (the most common one observed after deposition [85]) (a), one pair of legs is rotated, leading to the crossed legs (CL) conformation (b). Then the other pair of legs is manipulated, creating the second PL conformation (c). After another CL conformation (d), the initial configuration (e) is achieved. As can be seen in the final STM image, this configuration is perfectly equivalent to the initial one. Hence, all possible conformations can be induced by this manipulation mode, which can hardly be done by the common modes that include strong repulsive forces.

This manipulation mode is non-destructive, neither for the tip nor for the molecule, because only attractive forces are used. The resulting high reliability leads to a very high rate of successful events of more than 99% and thus enables the same conformational change on the same single molecule to be repeated many (>100) times (a movie is available in the supporting information of [78]). Notice that in a repulsive mode (as for the Cu-TBPP molecule discussed in figure 3.1 above), pushing on a leg holds the risk of damaging the STM tip and/or the molecule because repulsive forces become very large at small distances. The presented manipulation mode is therefore of great interest for a detailed understanding of the interatomic forces present during molecular manipulation, because one and the same molecule must be manipulated many times to allow parameter analysis. The use of manipulation data from different molecules would smear out the characteristic values, because the potential barrier height and thus the required threshold tip height can change from one molecule to the other, due to the local atomic environment at the step edge. It is therefore important to study the dependence of the process on the manipulation parameters always for one and the same molecule within one series.

The tip height, at which the manipulation process occurs during the approach, turns out to be characteristic for the conformational change. By analysing many equivalent manipulation processes (of a conformational change PL to CL) a threshold value of Δz is determined (with respect to the starting tip height of about 7 Å), below which (i.e. at larger tip heights) no conformational change can be induced. The dependence of the quantum yield, i.e. the number of events per tunnelling electron, on the lateral distance d_o between tip and leg in the $[1\bar{1}0]$ direction (defined in figure 3.7) shows a maximum at about 4 Å [78]. This value is therefore used in all manipulation series. The dependence of the quantum yield on the bias voltage reveals values of more than 10^{-10} events/electrons at voltages above 150 mV (at a fixed tip height: $\Delta z = 3$ Å), while no conformational change can be induced at voltages below 50 mV. A threshold voltage of 110 ± 30 mV is determined, showing that the manipulation process depends not only on the tip apex–molecule distance, but also on the bias voltage.

The fact that the tip has to be approached in front of the molecule points to a directional force driving the manipulation. This observation is confirmed when the STM tip is positioned at various angles θ off the $[1\bar{1}0]$ direction, always at the same height and lateral distance from the molecular leg to be manipulated, leaving the tunnelling current constant. While at large θ no conformational change can be induced, the quantum yield rises at smaller θ, revealing a maximum when the tip apex is positioned in front of the molecule. Furthermore, it turns out that the quantum yield is smaller (the current is larger as the tip must be closer to the surface) for conformational changes from crossed to parallel legs than for the opposite direction (PL to CL), due to the higher barrier for this conformational change (see figure 3.6(b)) and therefore need of larger forces [78].

As the driving force of the manipulation is directional and depends both on the tip height and the bias voltage, the process is likely driven by the electric field in the junction. It is known that electric-field-induced forces come into play when working with an STM [10]: electric-field-induced diffusion requires permanently charged atoms or molecules [97] while interaction between the electric field and a dipole occurs when a local

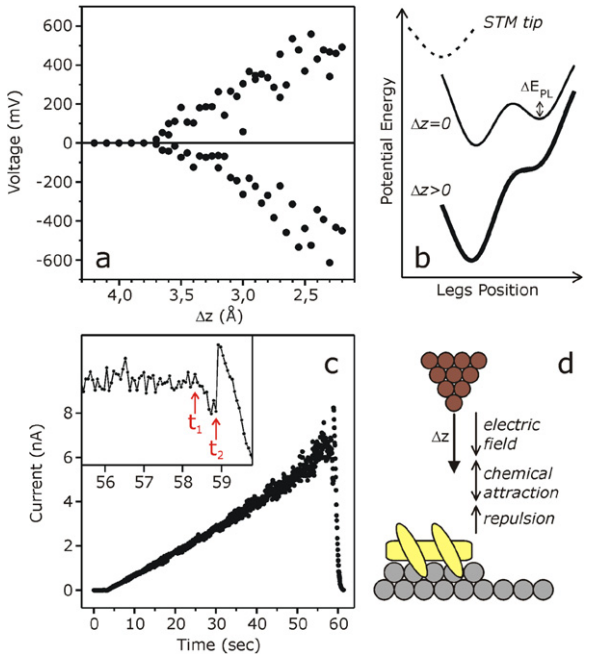

Figure 3.9. (a) Threshold voltage as a function of the vertical tip feed Δz of the manipulation process (for the conformational change from parallel to crossed legs for one and the same molecule). (b) Corresponding schematic potential energy curve. Dashed curve: tip-induced potential well; solid line: molecular legs without tip; Bold solid line: molecular legs in the presence of the STM tip ($\Delta z > 0$; meaning the tip is approaching the surface), i.e. the sum of the tip-induced potential well and the double-well potential of the molecule without a tip influence ($\Delta z = 0$). (c) Current signal during a conformational change from CL to PL at $\Delta z = 4.5$ Å. The inset shows an enlarged region with the important moments of tip retraction (t_1) and successful manipulation (t_2) visible as an abrupt current increase. Lines are drawn to guide the eyes. (d) Scheme of the three observed regimes of interatomic forces (at different tip heights). Reprinted with permission from [78]. Copyright (2006) American Chemical Society.

dipole moment is induced in the adsorbate [68]. The studied Lander molecules exhibit no permanent dipole moment. The presented experimental results are thus interpreted by the electric field which induces a dipole moment in the molecular legs [78]. The conformational change is achieved by the electrostatic force acting on them in the presence of the electric field in the STM junction.

To confirm this interpretation, the threshold voltage is determined as a function of the tip height (figure 3.9(a)). Each data point corresponds to one single manipulation process, where (at a given Δz) the bias voltage is raised slowly until the conformational change occurs. The result shows that the conformational change can be successfully induced over a tip height range of 3 Å. The necessary bias voltage changes in this range and reveals an approximately linear relationship between the tip–molecule distance and the applied voltage if Δz is below 3.7 Å. This dependence demonstrates the dipole–electric field interaction character. Ideally, the relationship between U and z should be linear, with a deviation at small tip heights. Notice that, above $\Delta z = 3.8$ Å, no bias voltage has to be applied for a successful PL to CL conformation change. The rotation of the legs is induced by positioning the tip at a sufficiently small tip height between the leg and the tip apex. Hence, chemical forces drive the intramolecular manipulation at these tip heights. Note that these chemical forces are *attractive*, in contrast to the case discussed above (figure 3.1).

The potential barrier between the two leg orientations drops upon the tip approach and ΔE_{PL} goes to zero (figure 3.9(b)), similar to the manipulation of single Co atoms on Cu(111) [98]. When inducing the opposite conformational change (from CL to PL), the threshold voltage does not go to zero but decreases to minimum values of ± 200 mV. This behaviour is due to the asymmetry of the double potential well profile, because the potential barrier is always present and ΔE_{CL} does not go to zero but reaches a constant (finite) value at very small tip heights [78].

It is not possible to determine a threshold voltage for Δz larger than 4.4 Å, because no rotation of the legs can be induced as long as the tip is very close. At $\Delta z = 4.5$ Å the current signal increases linearly (figure 3.9(c)), because the bias voltage is raised from 0 mV to -300 mV and exhibits no jump until the tip is retracted (at time t_1). However, an abrupt increase in the current signal is observed immediately afterwards (at time t_2). This shows that the small distance between tip and molecular leg suppresses the conformational change by hindering the leg to rotate, but as soon as the tip apex is out of this repulsive force range the conformational change of the molecule occurs.

An important observation that points against inelastic tunnelling processes, which could induce the conformational changes together with a deformation of the potential landscape upon the tip approach, is made at high tunnelling voltages. It has been checked if larger bias voltages can induce the conformational change when the tip is not positioned in front of the molecular leg. It turned out that no conformational change can be induced at all (at tip heights in the Δz range of -2 to $+3$ Å and resulting currents up to 25 nA) if the tip is positioned sideways or above the molecular leg, even at voltages up to 3 V [78]. Instead, the tip apex is modified or the molecule slightly changes its lateral position (retaining its conformation) or even dissociates.

These experiments show that it is possible to induce all possible conformational changes to the molecules with very high precision and reliability. Various interatomic forces, active during molecular manipulation, are characterized (figure 3.9(d)): at large tip heights electrostatic forces on the dipole moment induced in a molecular leg are invoked while chemical forces are observed when approaching the tip (no bias voltage necessary). In addition to these attractive forces, the regime of repulsive forces is reached at very small tip heights.

Finally, it should be mentioned that even molecules, which exhibit only one stable conformation when adsorbed on a surface, can undergo an intramolecular change if an STM tip is approached sufficiently, because they are compressed if the necessary repulsive forces are applied with the STM tip. However, such a modified structure is unstable in the absence of the STM tip and the process does therefore not represent an intramolecular manipulation between stable states. Figure 3.10

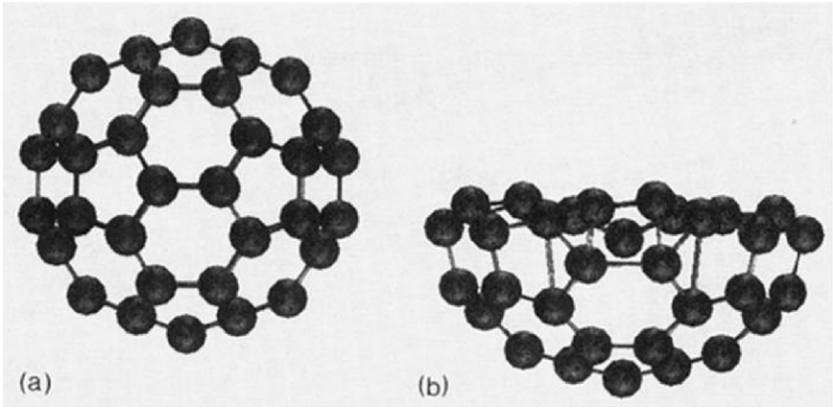

Figure 3.10. Calculated structure of a C_{60} molecule in the tunnelling junction for a tip apex to surface distance of (a) 14 Å and (b) 7.35 Å. The W tip apex was considered rigid during the approach. Reprinted with permission from [100]. Copyright (1995) by the American Physical Society.

shows an example, where the configuration of a fullerene molecules in a tunnelling junction has been calculated for different tip–surface distances. When the tip is far away (a), the C_{60} molecule maintains its stable structure, but when the tip is approached (b), it is strongly deformed. However, a more recent study of the same system, proposing that the molecule remains almost spherical with only small relaxations of carbon–carbon bonds, is in contradiction to this result [99].

4. Conclusions

It has been shown that the deposition of organic molecules onto a surface under ultrahigh vacuum conditions is not a trivial task if the molecules exceed a certain size. Such conditions are easily reached if specific functions are incorporated into a molecule. Furthermore, the use of low temperatures during the measurements enables the visualization of solvent molecules, which diffuse at room temperature. The presented techniques differ, on the one hand, in their complexity and the required experimental effort and, on the other hand, in the cleanliness and precision of the preparation. It is thus necessary to choose the best method, suitable for the available experimental set-up and required for the scientific question. In the future, it will be of interest to improve the control over the molecular coverages with these methods. At the moment, it is still difficult to predict a molecular coverage from the experimental deposition parameters, although this would be an important condition for a quick and easy deposition technique. In particular, if single molecules should be studied, it is necessary to deposit very small amounts of molecules in the sub-monolayer regime with high precision.

In the second part of this review, several examples of intramolecular manipulation by directional forces are presented. Different studies exist, where the conformation of a molecule has been changed without the use of inelastic tunnelling effects and without a lateral dislocation. In particular, the latter condition is important, because a lateral motion would be accompanied by a change in the adsorption site on the surface and thus a possible modification of the potential barriers for conformational changes. By using chemical or electrostatic forces, molecular side groups (i.e. legs) could be rotated, the internal configuration was modified and isomerization processes were induced reversibly. In particular, the case of a leg rotation of a so-called Lander molecule turns out to be very interesting, because very high rates of success of more than 99% could be achieved. Such a reliable manipulation process allows a detailed study of the present interatomic forces and the intramolecular changes. This is a very specific case though and for future experiments it would be of interest to apply this technique to a wider range of molecules. By reliably performing intramolecular manipulation with a high rate of success, the influence of the surface or of specific molecular side groups on the conformational changes could be studied systematically.

Acknowledgments

I want to thank my co-workers at the Freie Universität Berlin and the Nanoscience Group of Christian Joachim at the CEMES-CNRS in Toulouse for the excellent collaboration and fruitful discussions. Financial support from the European Union, through the projects AMMIST and PICO-INSIDE, and the German Science Foundation (DFG), through SFB 658 and GR 2697/1, is gratefully acknowledged.

References

[1] Joachim C and Gimzewski J K 2001 *Struct. Bond.* **99** 1
[2] Browne W R and Feringa B L 2006 *Nat. Nanotechnol.* **1** 25
[3] Binnig G, Rohrer H, Gerber C and Weibel E 1982 *Phys. Rev. Lett.* **49** 57
[4] Avouris P 1995 *Acc. Chem. Res.* **28** 95
[5] Meyer G, Repp J, Zöphel S, Braun K-F, Hla S W, Fölsch S, Bartels L, Moresco F and Rieder K-H 2000 *Single Mol.* **1** 79
[6] Moresco F 2004 *Phys. Rep.* **399** 175
[7] Hla S-W 2005 *J. Vac. Sci. Technol.* B **23** 1351
[8] Grill L 2008 *J. Phys.: Condens. Matter* **20** 053001
[9] Eigler D M and Schweizer E K 1990 *Nature* **344** 524
[10] Stroscio J A and Eigler D M 1991 *Science* **254** 1319
[11] Bartels L, Meyer G and Rieder K-H 1997 *Phys. Rev. Lett.* **79** 697
[12] Jung T A, Schlittler R R, Gimzewski J K, Tang H and Joachim C 1996 *Science* **217** 181

[13] Beton P H, Dunn A W and Moriarty P 1995 *Appl. Phys. Lett.* **67** 1075
[14] Selvanathan S, Peters M V, Schwarz J, Hecht S and Grill L 2008 *Appl. Phys.* A **93** 247
[15] Grill L, Dyer M, Lafferentz L, Persson M, Peters M V and Hecht S 2007 *Nat. Nanotechnol.* **2** 687
[16] Heinrich A J, Lutz C P, Gupta J A and Eigler D M 2002 *Science* **298** 1381
[17] Bouju X, Joachim C, Girard C and Tang H 2001 *Phys. Rev.* B **63** 085415
[18] Whitman L J, Stroscio J A, Dragoset R A and Celotta R J 1991 *Science* **251** 1206
[19] Bouju X, Devel M and Girard C 1998 *Appl. Phys.* A **66** S749
[20] Rezaei M A, Stipe B C and Ho W 1999 *J. Chem. Phys.* **110** 4891
[21] Meyer G, Bartels L and Rieder K-H 2001 *Comput. Mater. Sci.* **20** 443
[22] Gadzuk J W 1995 *Surf. Sci.* **342** 345
[23] Stipe B C, Rezaei M A and Ho W 1998 *Science* **279** 1907
[24] Lastapis M, Martin M, Riedel D, Hellner L, Comtet G and Dujardin G 2005 *Science* **308** 1000
[25] Stipe B C, Rezaei M A and Ho W 1998 *Phys. Rev. Lett.* **81** 1263
[26] Iancu V and Hla S-W 2006 *Proc. Natl Acad. Sci.* **103** 13718
[27] Alemani M, Selvanathan S, Moresco F, Rieder K-H, Ample F, Joachim C, Peters M V, Hecht S and Grill L 2008 *J. Phys. Chem.* C **112** 10509
[28] Iancu V, Deshpande A and Hla S-W 2006 *Nano Lett.* **6** 820
[29] Ho W 2002 *J. Chem. Phys.* **117** 11033
[30] Stipe B C, Rezaei M A, Ho W, Gao S, Persson M and Lundqvist B I 1997 *Phys. Rev. Lett.* **78** 4410
[31] Hla S-W, Bartels L, Meyer G and Rieder K-H 2000 *Phys. Rev. Lett.* **85** 2777
[32] Liljeroth P, Repp J and Meyer G 2007 *Science* **317** 1203
[33] Katano S, Kim Y, Hori M, Trenary M and Kawai M 2007 *Science* **316** 1883
[34] Repp J, Meyer G, Stojkovic S, Gourdon A and Joachim C 2005 *Phys. Rev. Lett.* **94** 026803
[35] Meyer G 1996 *Rev. Sci. Instrum.* **67** 2960
[36] Kuck S, Wienhausen J, Hoffmann G and Wiesendanger R 2008 *Rev. Sci. Instrum.* **79** 083903
[37] Joachim C, Gimzewski J K and Aviram A 2000 *Nature* **408** 541
[38] Beuhler R J, Flanigan E, Greene L J and Friedman L 1974 *J. Am. Chem. Soc.* **96** 3990
[39] Zambelli T, Jiang P, Lagoute J, Grillo S E, Gauthier S, Gourdon A and Joachim C 2002 *Phys. Rev.* B **66** 075410
[40] Rapenne G, Grill L, Zambelli T, Stojkovic S M, Ample F, Moresco F and Joachim C 2006 *Chem. Phys. Lett.* **431** 219
[41] Jimenez-Bueno G and Rapenne G 2003 *Tetrahedron Lett.* **44** 6261
[42] Grill L, Rieder K-H, Moresco F, Jimenez-Bueno G, Wang C, Rapenne G and Joachim C 2005 *Surf. Sci.* **584** L153
[43] Grill L, Rieder K-H, Moresco F, Rapenne G, Stojkovic S, Bouju X and Joachim C 2007 *Nat. Nanotechnol.* **2** 95
[44] Kanno T, Tanaka H, Nakamura T, Tabata H and Kawai T 1999 *Japan. J. Appl. Phys.* **38** 606
[45] Kasai H, Tanaka H, Okada S, Oikawa H, Kawai T and Nakanishi H 2002 *Chem. Lett.* **31** 696
[46] Terada Y, Choi B-K, Heike S, Fujimori M and Hashizume T 2003 *Nano Lett.* **3** 527
[47] Terada Y, Choi B-K, Heike S, Fujimori M and Hashizume T 2003 *Japan. J. Appl. Phys.* **42** 4739
[48] Terada Y, Choi B-K, Heike S, Fujimori M and Hashizume T 2003 *J. Appl. Phys.* **93** 10014
[49] Bernard R, Huc V, Reiss P, Chandezon F, Jegou P, Palacin S, Dujardin G and Comtet G 2004 *J. Phys.: Condens. Matter* **16** 7565
[50] Zambelli T, Boutayeb Y, Gayral F, Lagoute J, Girdhar N K, Gourdon A, Gauthier S, Blanco M-J, Chambron J-C, Heitz V and Sauvage J-P 2004 *Int. J. Nanosci.* **3** 331
[51] Grill L, Stass I, Rieder K-H and Moresco F 2006 *Surf. Sci.* **600** L143
[52] Moresco F, Meyer G, Rieder K-H, Ping J, Tang H and Joachim C 2002 *Surf. Sci.* **499** 94
[53] Jung T A, Schlittler R R and Gimzewski J K 1997 *Nature* **386** 696
[54] Yamada T, Shinohara H, Maofa G, Mashiko S and Kimura K 2003 *Chem. Phys. Lett.* **370** 132
[55] Saywell A, Magnano G, Satterley C J, Perdigao L M A, Champness N R, Beton P H and O'Shea J N 2008 *J. Phys. Chem.* C **112** 7706
[56] Rauschenbach S, Stadler F L, Lunedei E, Malinkowski N, Koltsov S, Costantini G and Kern K 2006 *Small* **2** 540
[57] Swarbrick J C, Taylor J B and O'Shea J N 2006 *Appl. Surf. Sci.* **252** 5622
[58] Satterley C J, Perdigao L M A, Saywell A, Magnano G, Rienzo A, Mayor L C, Dhanak V R, Beton P H and O'Shea J N 2007 *Nanotechnology* **18** 455304
[59] Yamada T, Suzuki H, Miki H, Maofa G and Mashiko S 2005 *J. Phys. Chem.* B **109** 3183
[60] Yamada T, Shinohara H, Maofa G, Kimura K and Mashiko S 2003 *Thin Solid Films* **438/439** 7
[61] Albrecht P M and Lyding J W 2003 *Appl. Phys. Lett.* **83** 5029
[62] Clair S, Rabot C, Kim Y and Kawai M 2007 *J. Vac. Sci. Technol.* B **25** 1143
[63] Grill L, Rieder K-H, Moresco F, Stojkovic S, Gourdon A and Joachim C 2005 *Nano Lett.* **5** 859
[64] Moresco F, Gross L, Grill L, Alemani M, Gourdon A, Joachim C and Rieder K-H 2005 *Appl. Phys.* A **80** 913
[65] Girard C, Bouju X and Joachim C 1992 *Chem. Phys.* **168** 203
[66] Moresco F, Meyer G, Rieder K-H, Tang H, Gourdon A and Joachim C 2001 *Phys. Rev. Lett.* **86** 672
[67] Weigelt S, Busse C, Petersen L, Rauls E, Hammer B, Gothelf K V, Besenbacher F and Linderoth T R 2006 *Nat. Mater.* **5** 112
[68] Qiu X H, Nazin G V and Ho W 2004 *Phys. Rev. Lett.* **93** 196806
[69] Yokoyama T, Yokoyama S, Kamikado T and Mashiko S 2001 *J. Chem. Phys.* **115** 3814
[70] Feringa B L 2001 *Molecular Switches* (Weinheim: Wiley–VCH)
[71] Rau H 2003 *Photochromism—Molecules and Systems* (Amsterdam: Elsevier) p 165
[72] Hagen S, Leyssner F, Nandi D, Wolf M and Tegeder P 2007 *Chem. Phys. Lett.* **444** 85
[73] Wolf M and Tegeder P 2009 *Surf. Sci.* **603** 1506
[74] Alemani M, Peters M V, Hecht S, Rieder K-H, Moresco F and Grill L 2006 *J. Am. Chem. Soc.* **128** 14446
[75] Dri C, Peters M V, Schwarz J, Hecht S and Grill L 2008 *Nat. Nanotechnol.* **3** 649
[76] Cembran A, Bernardi F, Garavelli M, Gagliardi L and Orlandi G 2004 *J. Am. Chem. Soc.* **126** 3234
[77] Gourdon A 1998 *Eur. J. Org. Chem.* **1998** 2797
[78] Grill L, Rieder K-H, Moresco F, Stojkovic S, Gourdon A and Joachim C 2006 *Nano Lett.* **6** 2685
[79] Langlais V J, Schlittler R R, Tang H, Gourdon A, Joachim C and Gimzewski J K 1999 *Phys. Rev. Lett.* **83** 2809
[80] Kuntze J, Berndt R, Jiang P, Tang H, Gourdon A and Joachim C 2002 *Phys. Rev.* B **65** 233405
[81] Rosei F, Schunack M, Jiang P, Gourdon A, Lagsgaard E, Stensgaard I, Joachim C and Besenbacher F 2002 *Science* **296** 328
[82] Schunack M, Rosei F, Naitoh Y, Jiang P, Gourdon A, Laegsgaard E, Stensgaard I, Joachim C and Besenbacher F 2002 *J. Chem. Phys.* **117** 6259

[83] Gross L, Moresco F, Alemani M, Tang H, Gourdon A, Joachim C and Rieder K-H 2003 *Chem. Phys. Lett.* **371** 750
[84] Moresco F, Gross L, Alemani M, Rieder K-H, Tang H, Gourdon A and Joachim C 2003 *Phys. Rev. Lett.* **91** 036601
[85] Grill L, Moresco F, Jiang P, Joachim C, Gourdon A and Rieder K-H 2004 *Phys. Rev.* B **69** 035416
[86] Alemani M, Gross L, Moresco F, Rieder K-H, Wang C, Bouju X, Gourdon A and Joachim C 2005 *Chem. Phys. Lett.* **402** 180
[87] Ge X, Kuntze J, Berndt R, Tang H and Gourdon A 2008 *Chem. Phys. Lett.* **458** 161
[88] Zambelli T, Tang H, Lagoute J, Gauthier S, Gourdon A and Joachim C 2001 *Chem. Phys. Lett.* **348** 1
[89] Otero R, Naitoh Y, Rosei F, Jiang P, Thostrup P, Gourdon A, Laegsgaard E, Stensgaard I, Joachim C and Besenbacher F 2004 *Angew. Chem. Int. Edn* **43** 2092
[90] Otero R, Rosei F, Naitoh Y, Jiang P, Thostrup P, Gourdon A, Laegsgaard E, Stensgaard I, Joachim C and Besenbacher F 2004 *Nano Lett.* **4** 75
[91] Otero R, Hümmelink F, Sato F, Legoas S B, Thostrup P, Laegsgaard E, Stensgaard I, Galvao D S and Besenbacher F 2004 *Nat. Mater.* **3** 779
[92] Zambelli T, Goudeau S, Lagoute J, Gourdon A, Bouju X and Gauthier S 2006 *ChemPhysChem* **7** 1917
[93] Yu M, Xu W, Benjalal Y, Barattin R, Laegsgaard E, Stensgaard I, Hliwa M, Bouju X, Gourdon A, Joachim C, Linderoth T R and Besenbacher F 2009 *Nano Res.* **2** 254
[94] Gross L, Moresco F, Savio L, Gourdon A, Joachim C and Rieder K-H 2004 *Phys. Rev. Lett.* **93** 056103
[95] Grill L and Moresco F 2006 *J. Phys.: Condens. Matter* **18** S1887
[96] Sautet P and Joachim C 1991 *Chem. Phys. Lett.* **185** 23
[97] Repp J, Meyer G, Olsson F E and Persson M 2004 *Science* **305** 493
[98] Stroscio J A and Celotta R J 2004 *Science* **306** 242
[99] Neel N, Kröger J, Limot L, Frederiksen T, Brandbyge M and Berndt R 2007 *Phys. Rev. Lett.* **98** 065502
[100] Joachim C, Gimzewski J K, Schlittler R R and Chavy C 1995 *Phys. Rev. Lett.* **74** 2102